

# Resonant x-ray scattering study of the antiferroelectric and ferroelectric phases in liquid crystal devices

L. S. Matkin, S. J. Watson, and H. F. Gleeson

*Department of Physics and Astronomy, University of Manchester, Manchester M13 9PL, United Kingdom*

R. Pindak and J. Pitney

*Bell Laboratories, Lucent Technologies, Murray Hill, New Jersey 07974*

P. M. Johnson and C. C. Huang

*School of Physics & Astronomy, University of Minnesota, Minneapolis, Minnesota 55455*

P. Barois

*Centre Recherche de Paul Pascal, CNRS, Bordeaux, France*

A.-M. Levelut

*University Paris Sud, Paris, France*

G. Srajer and J. Pollmann

*APS, Argonne National Laboratory, Argonne, Illinois 60439*

J. W. Goodby and M. Hird

*Department of Chemistry, Hull University, Hull HU6 7RJ, United Kingdom*

(Received 19 March 2001; published 18 July 2001)

Resonant x-ray scattering has been used to investigate the interlayer ordering of the antiferroelectric and ferroelectric smectic  $C^*$  subphases in a device geometry. The liquid crystalline materials studied contain a selenium atom and the experiments were carried out at the selenium  $K$  edge allowing x-ray transmission through glass. The resonant scattering peaks associated with the antiferroelectric phase were observed in two devices containing different materials. It was observed that the electric-field-induced antiferroelectric to ferroelectric transition coincides with the chevron to bookshelf transition in one of the devices. Observation of the splitting of the antiferroelectric resonant peaks as a function of applied field also confirmed that no helical unwinding occurs at fields lower than the chevron to bookshelf threshold. Resonant features associated with the four-layer ferroelectric liquid crystal phase were observed in a device geometry. Monitoring the electric field dependence of these ferroelectric resonant peaks showed that the chevron to bookshelf transition occurs at a lower applied field than the ferroelectric to ferroelectric switching transition.

DOI: 10.1103/PhysRevE.64.021705

PACS number(s): 61.30.-v

## INTRODUCTION

Ferroelectric liquid crystals are perhaps best known for their significant technological potential in fast, bistable devices [1]. The most common ferroelectric liquid crystal phase is the chiral smectic- $C$  phase ( $SmC^*$ ) in which rodlike molecules lie in layers with their average direction of orientation (the director) tilted with respect to the layer normal by a temperature dependent tilt angle ( $\theta_T$ ). The layer average dipole moment, which contributes to the spontaneous polarization that is characteristic of ferroelectric materials, is orthogonal to both the director and layer normal. The direction of tilt of the molecules, and hence the layer dipole moment, is approximately the same on progressing from one layer to the next, modified only by the influence of the macroscopic helicoidal structure the pitch of which is typically hundreds of layers.

Antiferroelectric liquid crystals [2] have recently been the focus of intense research, partly because of their significant potential for application in devices. The antiferroelectric li-

quid crystal phase ( $SmC_A^*$ ), is also helicoidal and is characterized by molecules in alternate layers tilting in opposite directions, the dipole contribution also reversing in direction from one layer to the next. Since the first observations of antiferroelectricity in liquid crystals, several different  $SmC^*$  subphases have been identified and studied [3]. The ferroelectric  $SmC_{F11}^*$  ( $F11$ ) and  $SmC_{F12}^*$  ( $F12$ ) phases can exist between the antiferroelectric  $SmC_A^*$  phase and the ferroelectric  $SmC^*$  phase. Another subphase, the  $SmC_\alpha^*$  phase, can exist between the  $SmC^*$  and the untilted smectic- $A$  ( $SmA$ ) phase. Each phase has a specific structure and all the phases differ significantly in their optical, electrical and electro-optic properties.

When ferroelectric materials are incorporated in devices their switching properties are found to depend on the layer geometry adopted within the device [1,4]. The layer geometry is similarly expected to have an influence on the properties of the other smectic subphases when constrained within a device. Interactions with the substrates and align-

ment layers can result in the formation of a chevron structure or other layer geometries, which in turn, influence electro-optic measurements in the  $\text{SmC}^*$  subphases. X-ray scattering has provided a wealth of information about the geometry of the smectic layers in devices and its deformation by electric fields [5–10], but the technique is not sensitive to differences in molecular arrangement from one layer to the next and cannot distinguish the different  $\text{SmC}^*$  subphases. Resonant x-ray scattering, however, can probe changes in molecular orientation and layer structure as a function of electric field where it is applied to materials in a device geometry.

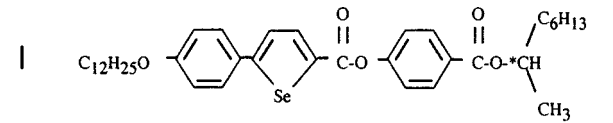
The interlayer ordering in molecular orientation for the  $\text{SmC}^*$  subphases is extremely difficult to study using most experimental techniques. Consequently, several different models of the antiferroelectric, ferrielectric, and ferroelectric phases have been proposed [11,12]. The resonant x-ray scattering technique is well established in the field of crystallography [13] and recently this method, combined with a polarization analysis of the x-ray features, gave support to a clocklike interlayer rotation of the tilt director being the most likely structure for the  $\text{SmC}^*$  subphases. Resonant x-ray scattering measurements directly revealed three and four layer periodicities in the  $F11$  and  $F12$  phases, respectively and a temperature sensitive periodicity of between five and eight layers in the  $\text{SmC}^*_\alpha$  phase [14,15]. Subsequent optical ellipsometry work [16] and further high-resolution x-ray resonant scattering studies [17] provide strong evidence for a distorted clock model.

The resonant scattering technique involves x-ray scattering at the absorption edge of an atom contained within the core of the liquid crystal molecule. Conventional x-ray scattering probes variations in electron density in the sample, whereby peaks are observed at  $Q_z = 2\pi l/d = lQ_0$ , where  $l$  is an integer and  $d$  is the smectic layer spacing. However, at the absorption edge energy the structure factor becomes a tensor [18] and the scattering becomes sensitive to molecular orientation. The value of the tensor is dependent on the orientation of the molecule with respect to the polarization direction of the x-ray beam, so extra peaks are observed where there is a periodicity associated with the interlayer tilt orientations and the different phases can be distinguished [19]. The resonant scattering features that have been resolved in the  $\text{SmC}^*$  subphases can be explained by assuming a constant interlayer rotation of magnitude  $2\pi(1/\nu + \varepsilon)$ , where  $\nu$  represents the superlattice periodicity and  $\varepsilon$  is the ratio of the smectic layer spacing to the optical pitch. This results in the observed resonant scattering peaks at

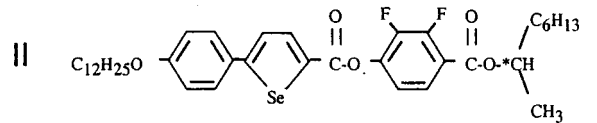
$$\frac{Q_z}{Q_0} = l + m(1/\nu + \varepsilon), \quad (1)$$

where  $l$  and  $m$  are integers and  $m = 0, \pm 1$  or  $\pm 2$ .

As already mentioned, the application of even small electric fields to devices containing the  $\text{SmC}^*$  subphases can result in changes in the macroscopic layer structure in addition to motion on a molecular level. The processes involved in such reorganizations are rather poorly understood, despite their importance in the application of antiferroelectric, ferrielectric, and ferroelectric liquid crystals in devices. This paper



**I**  
K 67.7  $\text{SmC}^*_A$  97.8  $\text{SmC}^*_{F11}$  99.0  $\text{SmC}^*$  109.4  $\text{SmA}$  116.6 **I**  
( $\text{SmI}^*$  33.3  $\text{SmI}^*_A$  42.2)



**II**  
K 46.3  $\text{SmC}^*_A$  82.6  $\text{SmC}^*_{F11}$  83.6  $\text{SmC}^*_{F12}$  86.3  $\text{SmC}^*$   
88.2  $\text{SmA}$  95.8 **I**

FIG. 1. The molecular structures and phase sequences for compounds I and II.

presents a study of the antiferroelectric and ferrielectric phases exhibited by two different liquid crystalline materials in a device geometry. The structural periodicity of the phases has been determined using resonant scattering at the selenium  $K$  absorption edge. This is a matter of considerable interest since the structure of the ferrielectric phases both in free-standing films and devices has, for several years, been a controversial subject. It is particularly crucial to confirm the existence and structure of the ferrielectric phases in bulk samples as liquid crystal films may exhibit different phases to those observed in the bulk geometry [20,21]. Further, a preliminary study of the antiferroelectric and ferrielectric structures under the influence of an electric field has been carried out. Resonant scattering features are presented as a function of applied electric field, and these data are correlated with electro-optic data for the same device. This work demonstrates the potential of the resonant scattering technique as a probe for switching studies in device geometries.

## EXPERIMENT

Resonant scattering has been performed on two different antiferroelectric liquid crystal materials, which have also been described elsewhere [22,23]. The molecular structures of the compounds are shown in Fig. 1 together with their phase sequences determined by a combination of optical microscopy, resonant scattering, and electro-optic techniques. Both molecules studied contain a selenium atom in their core and their molecular structures are very similar; compound II is a fluorinated version of compound I. The phase sequences are also similar; both materials exhibit antiferroelectric, ferroelectric, and at least one ferrielectric phase, confirmed by resonant scattering to be  $F11$  for compound I [24]. Microscopy of samples of compound II indicates the presence of two ferrielectric phases and since the higher temperature phase was shown to be  $F12$  by resonant scattering on a free-standing film [17], the lower temperature phase was assigned as  $F11$ .

X-ray experiments were carried out on beamlines 11D and 1BM at the Advanced Photon Source (APS) at Argonne National Laboratory. A synchrotron source is required in this

experiment for its high flux, polarization properties, and potential for energy selection.

In order to detect a resonant scattering signal, the x-ray beam was tuned to the  $K$  absorption edge of the selenium atom in the molecular core. The absorption edge was determined precisely by measuring fluorescence spectra emissions. It is important to note that this work is made possible by the use of materials containing a selenium atom. Previous resonant scattering work on free-standing films has mainly focused on sulphur containing materials but in order to see scattering from materials encased in glass, higher energies are required. The selenium  $K$  edge is at 12.66 keV, where the attenuation length in glass is about  $500 \mu\text{m}$ , while the sulphur  $K$  edge at 2.472 keV gives an attenuation length in glass of less than  $5 \mu\text{m}$ . The angular resolution of the experiment was defined by a Ge(111) analyzer.

The devices used were constructed of  $170 \mu\text{m}$  thick, indium-tin-oxide (ITO) coated glass. The inner surfaces of the glass plates that formed the device were spin coated with a thin nylon 6/6 alignment layer which was rubbed using a soft cloth to encourage uniform planar alignment of the liquid crystal molecules. The glass plates were assembled to enclose a  $15\text{--}30 \mu\text{m}$  thick liquid crystal sample, defined by the use of a polyethyleneterephthalate spacer. The device was capillary filled with liquid crystal and sealed using epoxy-resin cement. The devices were sufficiently thick to ensure that the helicoidal property of the liquid crystal was not suppressed. The conductive properties of the ITO coating in the device provided electrodes, thus allowing the application of electric fields across the liquid crystal up to  $5 \text{ V}/\mu\text{m}$ .

The device under investigation was mounted onto a heating stage connected to a remote temperature controller. The system provided temperature control of the sample with a relative accuracy of  $\pm 0.05 \text{ K}$ . When filled with a SmA material, a device such as described above will have a bookshelf geometry. In this geometry the smectic layers lie perpendicular to the glass surfaces. When a liquid crystal device cools from a nontilted smectic phase into a tilted one, the smectic layers usually buckle to form a chevron structure. In order to observe x-ray scattering from the liquid crystal layers in this geometry, the sample must be rocked to the chevron angle,  $\theta_C$ , as shown schematically in Fig. 2.

## RESULTS

### The antiferroelectric phase

The resonant scattering features associated with the antiferroelectric phase occur as additional peaks at positions where  $Q_z/Q_0 = (0.5 \pm \varepsilon)$ ,  $(1.5 \pm \varepsilon)$ , etc. Such peaks were observed in the antiferroelectric phases of both compounds I and II in devices held in the apparatus at the chevron angle. Typical resonant peaks obtained at  $Q_z/Q_0 = 0.5 \pm \varepsilon$  for compound I are shown in Fig. 3(a). Improvements to the scattering technique, including a better device alignment and thicker samples, have now significantly improved the signal to noise ratio compared with results published previously for compound I [24] and the much cleaner resonant peaks observed are apparent in the figure. The data presented in Fig. 3 were obtained from a device cooled directly to the antiferro-

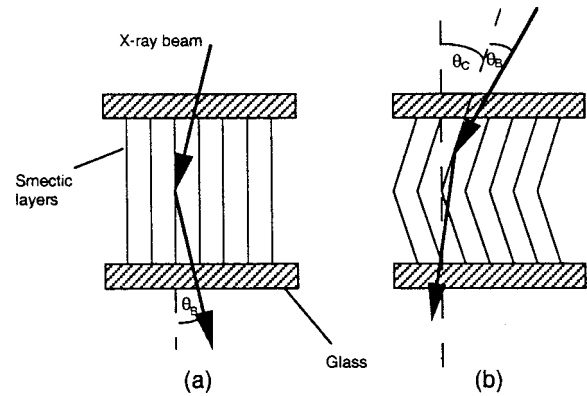


FIG. 2. Schematic of the scattering geometry for a liquid crystal device with (a) a bookshelf layer geometry and (b) a chevron layer geometry.  $\theta_C$  indicates the chevron angle and  $\theta_B$  is the Bragg scattering angle.

electric phase from the SmA phase, without the application of an electric field. Equation (1) indicates a splitting of the first order ( $m = \pm 1$ ) satellite peaks equal to  $2\varepsilon = 2d/P_0$  where  $d$  is the smectic layer spacing measured from the integer order layer peak positions and  $P_0$  is the optical pitch. The optical pitch of the  $\text{SmC}_A^*$  phase at  $85^\circ\text{C}$  deduced from these data is  $0.55 \mu\text{m}$ , a result in excellent agreement with that of the free-standing film data ( $0.58 \mu\text{m}$ ) at the same temperature. Antiferroelectric peaks were also observed for compound II [Fig. 3(b)]. The pitch deduced from these data, obtained at  $75^\circ\text{C}$ , is  $0.24 \mu\text{m}$ . It is interesting to note that the

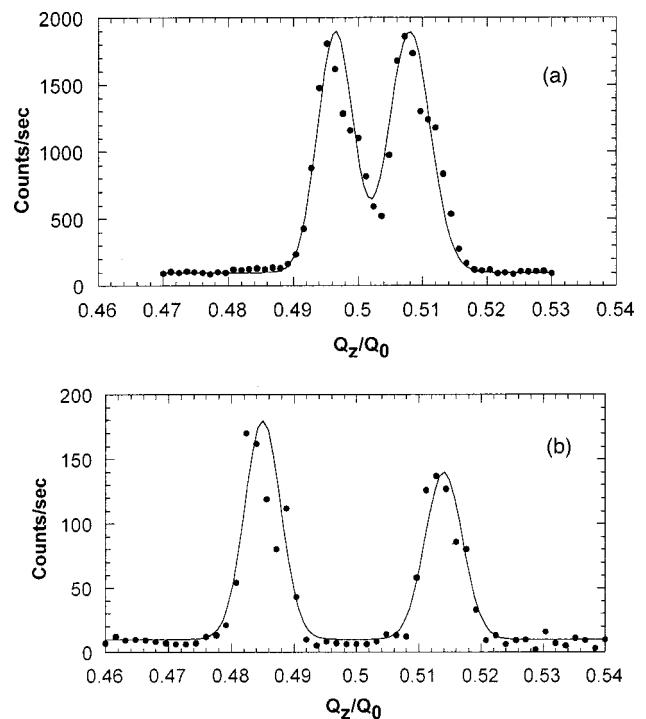


FIG. 3. Resonant peaks in the antiferroelectric phase at  $Q_z/Q_0 = 0.5 \pm \varepsilon$  for (a) compound I ( $85^\circ\text{C}$ ) and (b) compound II ( $75^\circ\text{C}$ ). The slight shoulder visible on each of these peaks is an experimental artifact and not related to the resonant signature of the material.

pitch in compound II is reduced by more than a factor of 2 from that of compound I just by the addition of two fluorine atoms to the molecular core.

Electric fields were applied to a liquid crystal device containing compound I using a 100-Hz ac square wave. Application of a field to the device allowed two different phenomena to be investigated. Field-induced changes to the pitch would be apparent from a change in the separation of the resonant peaks at  $Q_z/Q_0 = 1.5 \pm \varepsilon$ , while the antiferroelectric to ferroelectric switching transition would result in a loss of the resonant peaks. The magnitude of the applied field was increased stepwise, allowing the investigation of helical unwinding at low fields through the separation of the resonant peaks. Data acquisition was triggered such that scattering data were collected only during the last 33.3 ms of the positive part of the field cycle for the pitch investigations. No field-induced change in pitch was observed prior to the field-induced chevron to bookshelf transition in compound I. This observation was reinforced by evidence from optical transmission studies carried out on a polarizing microscope. The light intensity transmitted by a device identical to that used in the x-ray experiments, held between crossed polarizers with the rubbing direction almost parallel to one of the polarizers, shows no change in optical transmission below the ferroelectric switching threshold, confirming the results from x-ray data.

The onset of antiferroelectric to ferroelectric switching was also monitored as a function of applied field through the resonant feature at  $Q_z/Q_0 = 1.5 \pm \varepsilon$ . Fields of successively higher magnitude were applied to the device until, at 2.11 V/ $\mu\text{m}$  a threshold was reached. Figure 4 shows that below this threshold the half order resonant peaks indicative of the antiferroelectric structure are present. The peak splitting is approximately constant for all the data, implying that the field was not distorting the helix. Further, rocking curves at these field strengths confirmed that the sample remained in a chevron geometry. Above the threshold of 2.11 V/ $\mu\text{m}$  the resonant peaks at  $Q_z/Q_0 = 1.5 \pm \varepsilon$  disappear and a rocking curve on  $\theta$  confirmed that the layers had transformed to a bookshelf geometry. These data are consistent with the chevron to bookshelf transformation occurring at the same threshold field as the antiferroelectric to ferroelectric switching transition for this system at 85 °C.

### The ferroelectric phase

Compound II exhibits an *F12* phase in addition to the *F11* phase present in both materials. In the *F12* phase, the first order ( $l=1$ ,  $m=-1$ ) resonant peak was observed using a 28- $\mu\text{m}$ -thick device at  $Q_z/Q_0 = 0.75 - \varepsilon$  (Fig. 5). This result demonstrates that, in a device geometry, compound II maintains the four-layer repeat structure previously observed in free-standing film work [17]. We were not able to observe resonant features corresponding to the *F11* phase structure in devices containing either material, though such features are observed in free-standing films. This could be because either the peaks are too weak or the temperature range of the phase is too narrow and more careful measurements are required.

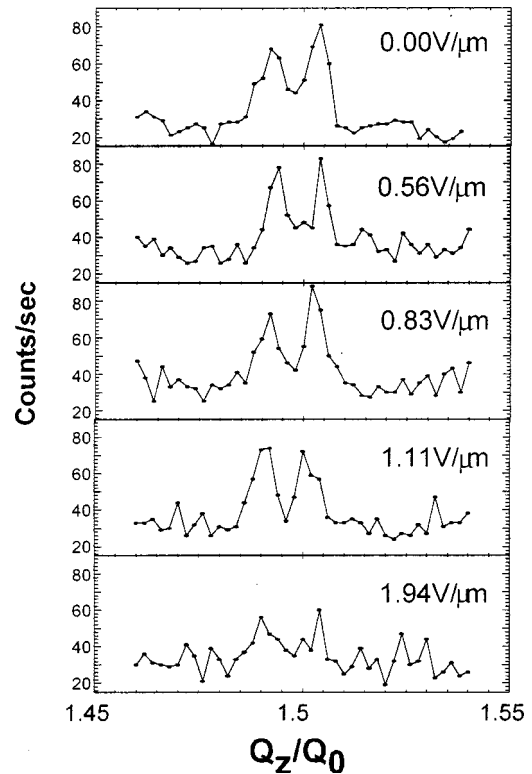


FIG. 4. The antiferroelectric resonant peaks at  $Q_z/Q_0 = 1.5 \pm \varepsilon$  under different applied electric fields (compound I, 85 °C).

Electric fields of gradually increasing amplitude were applied to the device with the liquid crystal in the *F12* phase. The ferroelectric resonant peak remains visible for applied fields as high as 0.71 V/ $\mu\text{m}$ , the maximum field applied (Fig. 6). For each different applied electric field the scattering signal from the  $Q_z/Q_0 = 1$  Bragg peak was optimized in  $\theta$  for the chevron angle (for voltages below that of the bookshelf transition). This optimization avoided the problem of moving out of the Bragg condition due to changes in chevron angle with field, a phenomenon observed to occur at relatively low fields in other ferroelectric materials [5]. With a 0.64 V/ $\mu\text{m}$  square wave applied, the ferroelectric peak is reduced in intensity, though this change can be explained by examining the rocking curve at this voltage. The chevron peaks are

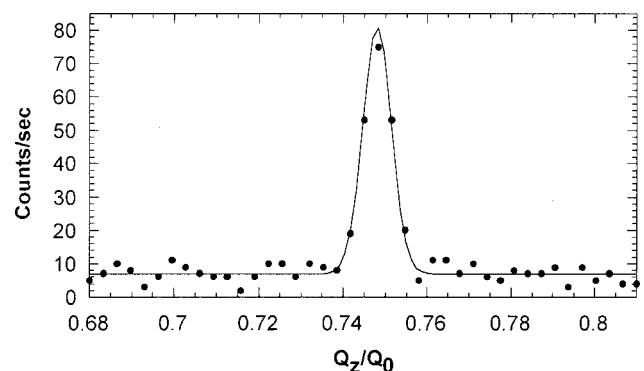


FIG. 5. The resonant peak in the *F12* phase of compound II at 86 °C.

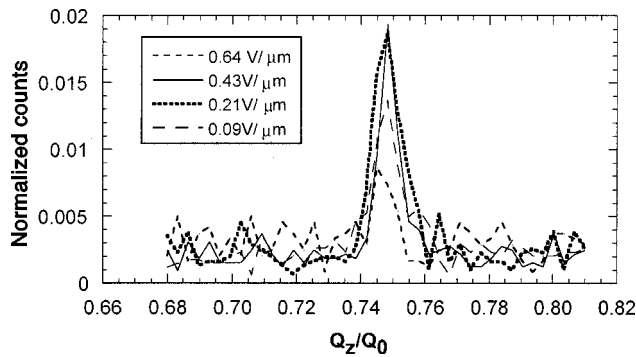


FIG. 6. The *F12* resonant peak with different applied electric fields at 86 °C. As there is some fluctuation in the scattering intensity over time these peak heights are represented as normalized counts, calculated as the ratio of the resonant peak height at  $Q_z/Q_0=0.75-\epsilon$  to the peak height at  $Q_z/Q_0=1$ .

broadened from a full width at half maximum of 2° at low voltages to 5° at 0.64 V/μm, thus reducing the  $Q_z/Q_0=1$  peak height by a factor of 2. After carrying out the resonant measurements, a field of 0.64 V/μm was kept on the sample for 26 min during which time further  $\theta$  rocking curves show that the sample gradually transformed from the chevron layer structure to a bookshelf geometry (Fig. 7). Persistence of the  $Q_z/Q_0=0.75$  resonant peak during the time evolution from chevron to bookshelf geometry indicates that the ferrielectric structure remains during and after this. When a higher electric field of 0.71 V/μm was then applied, an intense bookshelf peak was formed. This peak only slightly degraded in shape after the field was removed and the ferri phase was also observable (Fig. 8). These observations imply that the chevron to bookshelf transition in compound II at this temperature for a device of 28 μm occurs at a lower applied voltage than the onset of ferroelectric switching. Optical transmission data on a 5 μm thick device for this phase show two distinct thresholds with increasing field (Fig. 9). The first of these thresholds at 0.7 V/μm corresponds to the chevron to bookshelf transition seen by x-ray scattering (at 0.71 V/μm). The second threshold at 1.3 V/μm appears to be the field-induced ferrielectric to ferroelectric transition.

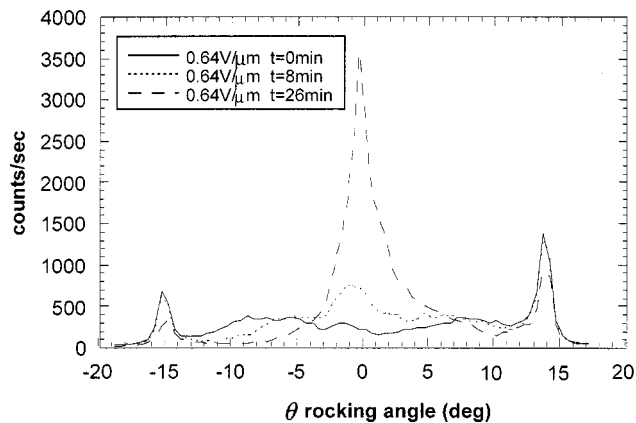


FIG. 7. Time evolution of the layer structure in the ferrielectric phase of compound II at 86 °C with 0.64 V/μm applied electric field.

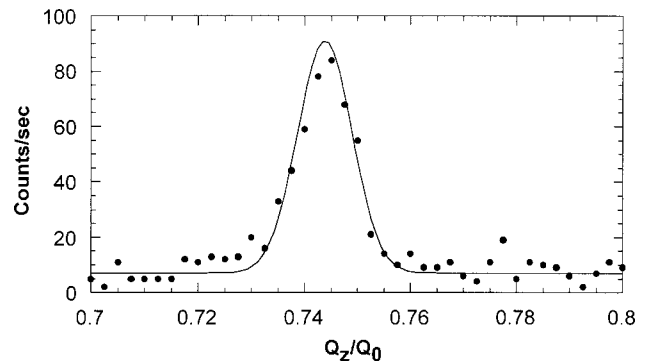


FIG. 8. Resonant peak in the four layer ferrielectric phase at 86 °C after the transition to a bookshelf structure and removal of the electric field.

CONCLUSIONS

In this paper a detailed investigation of the extent to which the technique of resonant scattering can be applied to devices has been carried out. Not only is it possible to identify and characterize phase structures in a material containing a suitable atom as previously reported, but it has been shown that it is also possible to probe electric field effects and structures within a liquid crystal device. In particular it has been demonstrated that the interlayer structures observable in a free standing film geometry also exist in the liquid crystal device.

The well known transition of the antiferroelectric phase to an unwound ferroelectric state on the application of a high electric field has been investigated and directly confirmed in this study. In compound I the antiferroelectric phase has been observed and the disappearance of antiferroelectric structure has been correlated with the onset of ferroelectric switching. It has also been confirmed that no helical unwinding occurs below the chevron to bookshelf transition. For compound II, the antiferroelectric phase has been observed and the ferrielectric phase structure has been confirmed within a device. In the ferrielectric phase a four-layer repeat structure, characteristic of a *F12* phase, was revealed as previously seen at the same temperature in films. Unfortunately, although the *F11* phase with a three-layer repeat structure occurs in both

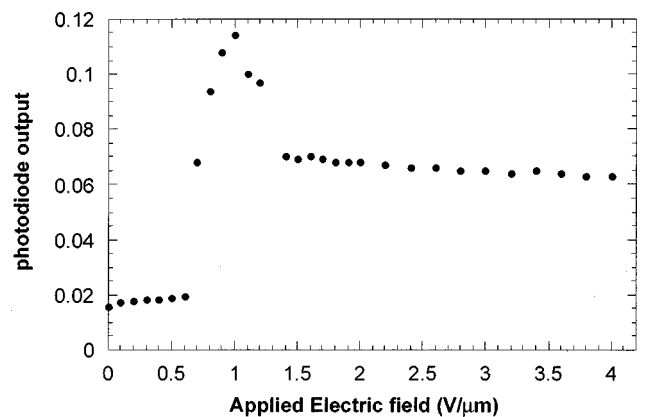


FIG. 9. Optical transmission as a function of applied electric field in the *F12* phase of compound II.

materials studied, it was not possible to observe resonant peaks for this phase in a device. If these samples undergo prolonged exposure to the x-ray beam, phase boundaries have been observed to decrease in temperature. The temperature range of the *F11* phase is narrow in both materials and may be particularly sensitive to this effect. The *F12* phase structure was monitored through the chevron to bookshelf transition using the  $Q_z/Q_0=0.75-\varepsilon$  resonant peak. This work demonstrates that in this material the *F12* four-layer repeat structure is retained despite layer rearrangements in the device. Perhaps surprisingly, the chevron to bookshelf transition was observed to occur at a lower applied field than that which induced ferroelectric switching. This observation has implications for the interpretation of electro-optic mea-

surements in the ferroelectric phase. Clearly parameters such as temperature, device thickness and material properties are likely to influence the field dependant behavior of antiferro- and ferroelectric phases, these considerations are a matter for future investigation.

Work at the Advance Photon Source was supported by the U.S. Department of Energy, Basic Energy Sciences, Office of Energy Research, under Contract No. W-31-109-ENG-38. L.S.M., H.F.G., and S.J.W. thank the EPSRC (GR/L/76648 and GR/R/19601) for financial support. L.S.M. thanks Lucent Technologies for additional financial support. R.P., P.M.J., and C.C.H. also acknowledge support from NSF-DMR-9901739. P.B. and A.M.L. acknowledge support from CNRS GDR606 and CNRS-NSF 99-7396.

- 
- [1] N. A. Clarke and S. T. Lagerwall, in *Ferroelectric Liquid Crystals—Principles, Properties and Application*, Ferroelectricity and Related Phenomena Vol 7 (Gordon and Breach Science Publishers, New York, 1991).
- [2] A. D. L. Chandani, E. Gorecka, Y. Ouchi, H. Takezoe, and A. Fukuda, *Jpn. J. Appl. Phys., Part 1* **28**, 1265 (1989).
- [3] A. Fukuda, Y. Takanishi, T. Isozaki, K. Ishikawa, and H. Takezoe, *J. Mater. Chem.* **4**, 997 (1994).
- [4] T. P. Reiker *et al.*, *Phys. Rev. Lett.* **59**, 2658 (1987).
- [5] L. S. Matkin, H. F. Gleeson, L. J. Baylis, S. J. Watson, and N. Bowring, *Appl. Phys. Lett.* **77**, 340 (2000).
- [6] P. Cluzeau, P. Barois, H. T. Nguyen, and C. Destrade, *Eur. Phys. J. B* **3**, 73 (1998).
- [7] J. S. Patel, Sin-Doo Lee, and J. W. Goodby, *Phys. Rev. A* **40**, 2854 (1989).
- [8] G. Srajer, R. Pindak, and J. S. Patel, *Phys. Rev. A* **43**, 5744 (1990).
- [9] M. Johno *et al.*, *Jpn. J. Appl. Phys., Part 2* **28(1)**, L119 (1989).
- [10] A. S. Morse, H. F. Gleeson, and S. Cummings, *Liq. Cryst.* **23**, 717 (1997).
- [11] K. Hiraoka *et al.*, *Jpn. J. Appl. Phys., Part 2* **30**, L1819 (1991); T. Isozaki *et al.*, *Jpn. J. Appl. Phys., Part 1* **31**, 1435 (1992).
- [12] M. Cepic and B. Zeks, *Mol. Cryst. Liq. Cryst. Sci. Technol., Sect. A* **263**, 61 (1995); V. L. Lorman, *ibid.* **262**, 437 (1995); S. A. Piken, S. Hiller, and W. Haase, *ibid.* **262**, 425 (1995); A. Roy and N. Madhusudana, *Europhys. Lett.* **36**, 221 (1996).
- [13] D. H. Templeton and L. K. Templeton, *Acta Crystallogr., Sect. A: Found. Crystallogr.* **A42**, 478 (1986).
- [14] P. Mach *et al.*, *Phys. Rev. E* **60**, 6793 (1999).
- [15] P. Mach *et al.*, *Phys. Rev. Lett.* **81**, 1015 (1998).
- [16] P. M. Johnson *et al.*, *Phys. Rev. Lett.* **84**, 4870 (2000).
- [17] L. S. Matkin, S. Watson, H. F. Gleeson, R. Pindak, J. Pitney, A. Cady, C. C. Huang, J. W. Goodby, M. Hird, and W. Caliebe (unpublished).
- [18] V. E. Dmitrienko, *Acta Crystallogr., Sect. A: Found. Crystallogr.* **A39**, 29 (1983).
- [19] A. M. Levelut and B. Pansu, *Phys. Rev. E* **60**, 6803 (1999).
- [20] E. B. Sirota, P. S. Pershan, L. B. Sorensen, and J. Collett, *Phys. Rev. A* **36**, 2890 (1987).
- [21] J. F. Li *et al.*, *Jpn. J. Appl. Phys., Part 1* **35**, 1608 (1996).
- [22] M. Hird *et al.*, *Mol. Cryst Liq. Cryst.* (to be published).
- [23] J. T. Mills *et al.*, *J. Mater. Chem.* **8**, 2385 (1998).
- [24] L. S. Matkin *et al.*, *Appl. Phys. Lett.* **76**, 1863 (2000).